

1-1-2006

One-dimensional transient analysis of volumetric heating for laser drilling

Chong Zhang
University of Central Florida

Islam A. Salama

Nathaniel R. Quick

Aravinda Kar
University of Central Florida

Find similar works at: <https://stars.library.ucf.edu/facultybib2000>
University of Central Florida Libraries <http://library.ucf.edu>

This Article is brought to you for free and open access by the Faculty Bibliography at STARS. It has been accepted for inclusion in Faculty Bibliography 2000s by an authorized administrator of STARS. For more information, please contact STARS@ucf.edu.

Recommended Citation

Zhang, Chong; Salama, Islam A.; Quick, Nathaniel R.; and Kar, Aravinda, "One-dimensional transient analysis of volumetric heating for laser drilling" (2006). *Faculty Bibliography 2000s*. 6754.
<https://stars.library.ucf.edu/facultybib2000/6754>

One-dimensional transient analysis of volumetric heating for laser drilling

Cite as: J. Appl. Phys. **99**, 113530 (2006); <https://doi.org/10.1063/1.2204828>

Submitted: 15 September 2005 . Accepted: 04 April 2006 . Published Online: 15 June 2006

Chong Zhang, Islam A. Salama, Nathaniel R. Quick, and Aravinda Kar



View Online



Export Citation

ARTICLES YOU MAY BE INTERESTED IN

[One-dimensional steady-state model for damage by vaporization and liquid expulsion due to laser-material interaction](#)

Journal of Applied Physics **62**, 4579 (1987); <https://doi.org/10.1063/1.339053>

[A model for self-defocusing in laser drilling of polymeric materials](#)

Journal of Applied Physics **103**, 014909 (2008); <https://doi.org/10.1063/1.2829818>

[Heating of solid targets with laser pulses](#)

Journal of Applied Physics **46**, 1585 (1975); <https://doi.org/10.1063/1.321760>

Lock-in Amplifiers up to 600 MHz

starting at

\$6,210



Zurich
Instruments

Watch the Video

One-dimensional transient analysis of volumetric heating for laser drilling

Chong Zhang

Department of Mechanical, Materials and Aerospace Engineering, College of Optics and Photonics, Center for Research and Education in Optics and Lasers (CREOL), University of Central Florida, Orlando, Florida 32816-2700

Islam A. Salama

Intel Corporation—Assembly and Technology Development, 5000 W. Chandler Boulevard, CH5-159, Chandler, Arizona 85226-3699

Nathaniel R. Quick

AppliCote Associates, LLC, 1445 Dolgner Place, Suite 23, Sanford, Florida 32771

Aravinda Kar^{a)}

College of Optics and Photonics, Center for Research and Education in Optics and Lasers (CREOL), University of Central Florida, Orlando, Florida 32816-2700

(Received 15 September 2005; accepted 4 April 2006; published online 15 June 2006)

Generally laser energy is considered to interact only with the substrate surface, as in metals, where the laser beam does not propagate into the substrate beyond a very small absorption depth. There are, however, many instances, particularly for ceramics and polymers, where the laser beam can penetrate into the substrate to substantial depths depending on the laser wavelength and laser-material interaction characteristics. Specifically there are polymeric dielectrics used as multilayer electronic substrates in which a laser beam of wavelength $9.3\ \mu\text{m}$ can penetrate into the substrate. The laser energy interacts at the substrate surface as well as inside the substrate. This particular aspect of laser-material interactions is important in laser drilling of blind microvias in polymeric multilayer electronic substrates. A one-dimensional transient heat conduction model including vaporization parameters is constructed to analyze this behavior. The absorption coefficient of the dielectric is also considered in this model and the problem is solved analytically. The microvia drilling speed, temperature distribution in the dielectric, and the thickness of the residue along the microvia walls and at the bottom of the microvia are studied for different laser irradiation conditions. An overheated metastable state of material is found to exist inside the workpiece. The overheating parameters are calculated for various laser drilling parameters and are used to predict the onset of thermal damage and to minimize the residue. © 2006 American Institute of Physics. [DOI: 10.1063/1.2204828]

I. INTRODUCTION

Lasers are extensively used to process various types of materials such as metals, semiconductors, polymers, and ceramics. A CO_2 laser of wavelength $9.3\ \mu\text{m}$ is widely used for microvia drilling in polymeric dielectrics to produce high density, multilayer, interconnect substrates. Although an excimer laser may seem to be appropriate for this application, the infrared (IR) laser is used because of its strong interaction with the molecules of the polymeric dielectric¹ and high throughput. More importantly, the embedded thin copper pads in multilayer substrates act as a drilling stopper because of the very high reflectivity of copper at the IR wavelength. The excimer lasers, on the other hand, may damage the thin pads by ablating the copper. However, the longer wavelengths of IR lasers make it difficult to produce microvias with small diameters. During laser drilling not only phase transitions (e.g., solid \rightarrow glassy phase \rightarrow melt \rightarrow vapor) occur but also chemical degradation of the polymer can occur before reaching the vaporization point.² To simplify the modeling approach, the chemical degradation can be treated as sublimation, because both processes absorb energy and give

off gases. The surface temperature quickly stabilizes after the chemical degradation of the polymer and tends to remain constant for different laser parameters.³ So the surface temperature, which is termed the thermal decomposition point, is considered to be constant in this study.

Unlike most metallic materials, which have an absorption length less than $0.1\ \mu\text{m}$ for the laser wavelength, polymeric materials allow deeper penetration of lasers at certain wavelengths.⁴ Usually the absorption depth l_v , which is given by $l_v \sim 1/\mu$ where μ is the absorption coefficient, of polymer is $10\ \mu\text{m}$.⁵ Phonons are created in the substrate after the laser energy is absorbed by the substrate molecules. These phonons conduct heat to various regions of the substrate. The characteristic length for the propagation of the thermal energy is given by the thermal influence length $l_T \sim \alpha/V$, where α is the thermal diffusivity and V is the velocity of the vaporization front.⁶ The relative magnitude of these two lengths defines whether volumetric laser heating is important for a given case of laser-matter interaction. A volumetric heating (V_h) number, which is a dimensionless number given by $V_h = V/\alpha\mu$, is defined in this study to express the relative importance of these two lengths. The volumetric heating is appreciable when $V_h \geq 1$. This condition is satis-

^{a)}Electronic mail: akar@creol.ucf.edu

fied for many polymeric dielectrics even for $V \sim 0.01$ m/s. So the drilling model must consider the laser heating and the removal of polymeric material due to volumetric heating. It has been confirmed experimentally that an analytic model based on volumetric heating is more accurate than a model based on surface heating.⁷

The volumetric heating creates an overheated metastable state with the maximum temperature occurring beneath the substrate surface,^{6,8,9} when the surface is maintained at a constant temperature, e.g., the vaporization temperature. This overheating induces phase transformation in the polymer. It also causes thermomechanical breakage of the material when the thermal stress exceeds a critical value, leading to material removal through explosion under certain laser parameters. Such an explosive material removal mechanism makes the drilling process unstable. Additionally, the overheating can produce a thicker heat-affected zone (HAZ) in the polymer. The HAZ, which will be referred to as “smear residue,” is formed in the region where the temperature exceeds the thermal decomposition point.¹⁰ Smear residue is formed along the walls of the hole and at the bottom of the embedded copper pad in multilayer copper-polymer structures.^{5,11}

Despite the above disadvantages, the explosive removal of polymeric material through the volumetric heating mechanism would be energetically more efficient than the conventional laser-polymer drilling which relies only upon the vaporization of the material. So the volumetric heating process needs to be studied to control the explosive removal of materials and to minimize or eliminate the formation of smear residue. The effects of volumetric heating on the quality of laser drilling depend on the thermophysical and optical properties of polymeric substrates as well as the laser beam parameters such as the irradiance and pulse duration. To improve the drilling efficiency, a short drilling time at high irradiance ($\sim 10^5$ W/cm²) is generally required. At high irradiances, however, the hot polymer vapor transforms into plasma,^{12–14} affecting the propagation of the laser beam through the plasma to the substrate. For materials having low vaporization temperature, the plasma formation is negligible when the irradiance is not excessively high.¹⁵

Most of the previous laser drilling models only considered the laser energy absorbed at the substrate surface.^{16–20} Dabby and Paek²¹ presented a transient one-dimensional model considering the penetration of radiation into the material. Noguchi *et al.*⁵ applied the enthalpy method to formulate a one-dimensional volumetric heating model and solved it using a finite element technique. Mazhukin *et al.*^{6,8} analyzed the overheating process by using a one-dimensional model. Sobol and Petrovskaya²² studied the high- T_c superconductor (HTSC) evaporation and decomposition due to volumetric heating.

In the present work, transient heat conduction model is developed to analyze the laser drilling process for polymeric substrates. An analytic method is used to study the effects of volumetric heating on the drilling front profile, drilling speed, and temperature distribution. The effects of the irradiance profile are also examined and the results are presented for a CO₂ laser of wavelength 9.3 μ m.

II. MATHEMATICAL MODEL

The occurrence of various optothermal processes due to laser-polymer interactions is described in Fig. 1. When a laser beam is incident on a substrate, a fraction of the laser energy penetrates into the substrate and is absorbed within a certain volume of the material resulting in volumetric heating. This will heat up the substrate first by supplying only the sensible heat up to a certain time t_h . At time $t=t_h$, the surface temperature reaches the vaporization point of the substrate. The latent heat of vaporization will be absorbed by the surface up to a certain time t_v , i.e., during the time period $t_h \leq t < t_v$ and overheating (i.e., temperature exceeding the vaporization point) starts inside the workpiece in this time period. At time $t=t_v$, the energy absorbed by the surface exceeds the latent heat of vaporization and a transient state of vaporization occurs up to a certain time t_{qs} , i.e., during $t_v \leq t < t_{qs}$. This vaporization process enables drilling of the substrate. As the drilling front moves, a quasisteady state is established at $t=t_{qs}$. During the quasisteady state ($t_{qs} \leq t < t_{on}$), where t_{on} is the pulse-on time, the overheating inside the polymer continues. A large portion of the polymer is vaporized in this period. During the laser pulse-off time ($t_{on} \leq t < t_p$, where t_p is the period of the laser pulses), vaporization continues due to the excess thermal energy in the overheated region inside the substrate. Depending on the amount of the excess energy, the volumetric heating may leave residue on the sidewalls and at the bottom corner of holes in polymeric substrates. The residue can be removed by using more pulses with annular irradiance profile. The overheating can also cause thermochemical damage to the substrate around the surface of the hole, and generate residual thermal stresses in the substrate. Explosive material removal occurs during the drilling process if the thermal stress exceeds the yield stress of the substrate.

The depth of the microvias is about 30 μ m. During the drilling process the thickness of the liquid layer would be a fraction of this depth. It is actually less than 0.5 μ m, if the laser intensity is larger¹⁵ than 3.69×10^4 W/cm². The laser intensity used to drill the polymer substrate is 1.2×10^6 W/cm². In this paper, which means thinner liquid phase.²³ The Peclet number, $Pe = \delta u_r / \alpha$, is a measure of the importance of heat convection relative to the heat conduction. Here δ is the thickness of the liquid layer, u_r is a characteristic velocity of the molten polymer, and α is the thermal diffusivity of the polymer. The value of u_r , which represents the radial velocity in this study, is estimated below to obtain Pe .

Three driving forces may be identified for the flow of molten polymer: (i) buoyancy force due to density difference, (ii) surface tension gradient due to temperature-dependent surface tension, and (iii) recoil pressure due to the outgoing vapor.²³ Because of the volumetric heating and thinness of the liquid layer, the temperature is expected to be uniform along the depth of the liquid layer and therefore the buoyancy force can be neglected. The surface tension gradient causes radial flow while the recoil pressure squeezes the liquid in the z direction (Fig. 2) to eventually cause radial flow.²³ An effective recoil pressure, $P_{\text{eff}} = (1/2)\rho V_{\text{eff}}^2$, may be

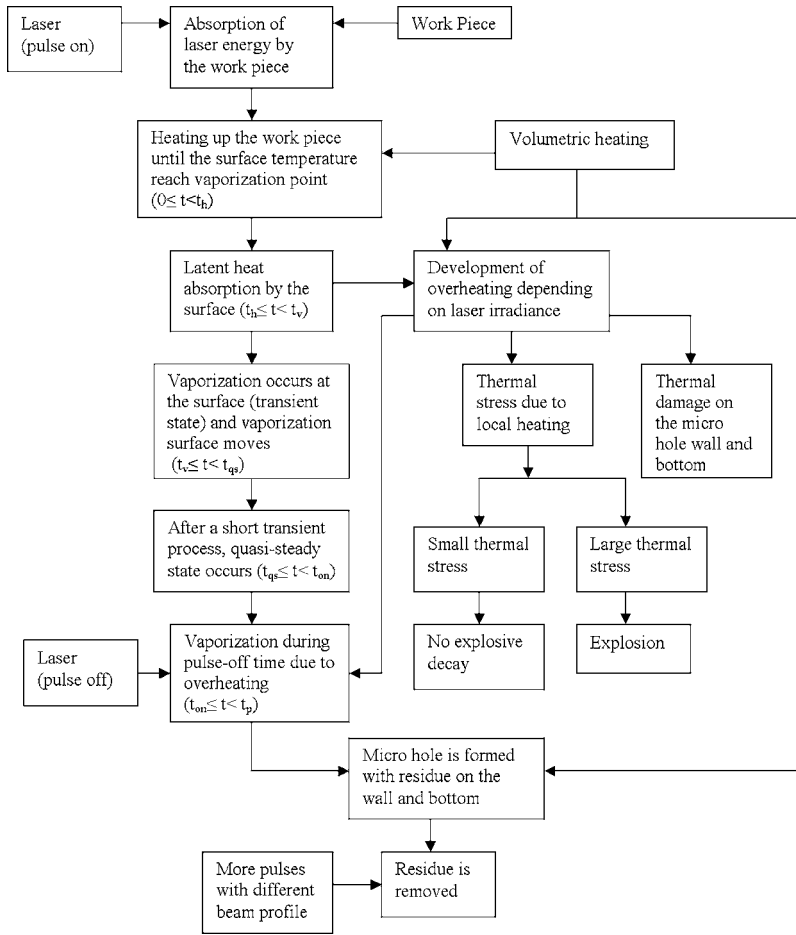


FIG. 1. A schematic representation of laser-polymer interaction process.

defined to combine the effects of these two driving forces in order to estimate u_r . Here V_{eff} is an effective vapor velocity representing the actual vapor velocity and an additional velocity whose recoil pressure produces the same effect on the polymer flow as the surface tension gradient. ρ is the density of the liquid polymer. The effective recoil pressure induces shear stress in the liquid polymer, i.e., $P_{\text{eff}} \approx \mu(du_r/dz)$, where the shear stress of Newtonian fluids has been considered, although polymers are generally non-Newtonian fluid, in order to estimate u_r . Here μ is the viscosity of the molten

polymer with typical values^{24,25} of 10^6 kg/(m s). Since δ is small, du_r/dz can be expressed as u_r/δ . So the above approximation leads to $u_r \approx (\delta/\mu)(1/2)\rho V_{\text{eff}}^2$.

Substituting the properties of the polymer into this expression, $u_r = 2.5 \times 10^{-10} V_{\text{eff}}^2$. If the effective velocity is taken as the speed of sound, i.e., $V_{\text{eff}} = 340$ m/s, the characteristic velocity of the liquid polymer is $u_r = 2.89 \times 10^{-5}$ m/s and the corresponding Peclet number $Pe = 5.78 \times 10^{-5}$ which is very small. Even if the effective vapor velocity V_{eff} corresponds to Mach number of 10, which is very small. So the convection in the molten polymer can be neglected.

A geometric configuration of the drilling model is shown in Fig. 2. A layer of copper covered with a layer of polymer on both sides is used to simulate the presence of embedded copper pads in actual multilayered substrates. The laser beam penetrates into the substrate during the pulse-on time and is absorbed by the substrate with an absorption coefficient μ . Assuming the Bouguer-Lambert law to be valid, the laser irradiance propagating downward inside the polymer can be expressed as

$$I_{ip} = I_i \exp(-\mu z), \tag{1}$$

where a moving coordinate system is considered with the origin of z being located at the drilling front $s(r, t)$, and I_i is the incident laser irradiance.

For a Gaussian beam,

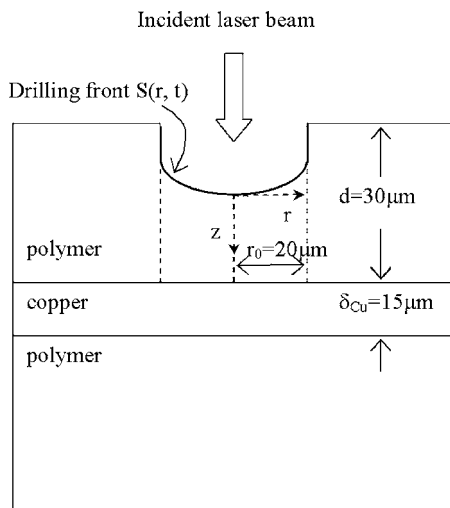


FIG. 2. Geometric configuration of drilling model.

$$I_i = (1 - R_{\text{poly}})I_0 \exp(-2r^2/r_0^2)\Phi(t), \quad (2)$$

where R_{poly} is the reflectance of the polymeric substrate and $\Phi(t)$ is the laser pulse shape function. I_0 is laser irradiance at the center of the beam, which is given by

$$I_0 = 2Pt_p/\pi r_0^2 t_{\text{on}}, \quad (3)$$

for a rectangular pulse shape considered in this study. Here P is the average laser power and r_0 is the radius of incident laser beam.

It is assumed that the laser beam does not penetrate the copper. Some of the laser power is absorbed by the top surface of the copper and the rest of the power is reflected. The irradiance of the reflected beam can be expressed as

$$I_r = R_{\text{Cu}}I_i \exp\{-\mu[d - s(r,t)]\}, \quad (4)$$

where R_{Cu} is the reflectance of copper.

The laser irradiance propagating upward inside the polymer can be written as

$$I_{rp} = I_r \exp\{-\mu[d - s(r,t) - z]\}. \quad (5)$$

Some of the laser energy would also be used to dissociate the polymer molecules. The photon energy of a CO₂ laser of wavelength 10.6 μm is 0.11 eV which is much lower than the bond energies of typical polymers such as 3.89 eV for C–C and 4.36 eV for C–H bonds in epoxy resin, respectively.²⁶ So the photolytic dissociation of the polymer molecules would not occur. Pyrolytic, i.e., thermal decomposition of the molecules, will occur. This effect is considered in the model through an effective value of the latent heat of vaporization which includes the breakage of long polymer chains into shorter chains during the vaporization process.

Based on these considerations for the downward and upward moving laser beams, a thermal model is developed for the drilling process under the following assumptions

- (1) The polymer material, such as the silica-filled epoxy polymers widely used as the organic high density interconnect substrates, is considered isotropic.
- (2) The thermophysical properties are independent of temperature.
- (3) Absorbed laser energy is converted to thermal energy instantaneously.
- (4) The heat will decompose the polymer, which is considered to occur only on the drilling front surface, and then vaporize it. The material removal is modeled as a sublimation process (solid-to-vapor phase transition) because of the short lifetime of the liquid phase.¹⁵
- (5) There is no plasma formation. The vapor is transparent to the incident laser beam.
- (6) The radiative heat loss is negligibly small compared to the heat conduction.
- (7) The heat, which conducts through the copper, produces a thermal diffusion layer in the polymer below the copper layer.

Because of the short time during which the polymer is heated until the surface temperature reaches the vaporization point,²⁷ the vaporization is considered to begin simultaneously as the laser irradiates the substrate. The transient

heat transfer process after the beginning of vaporization can be described by the following governing equation in a cylindrical coordinate system moving with the vaporization (i.e., drilling) front:

$$\frac{1}{r} \frac{\partial}{\partial r} \left(r \frac{\partial T}{\partial r} \right) + \frac{\partial^2 T}{\partial z^2} + \frac{g}{k} = \frac{1}{\alpha} \left[\frac{\partial T}{\partial t} - \frac{\partial T}{\partial z} \frac{\partial s(r,t)}{\partial t} \right], \quad (6)$$

for $0 < z < d - s(r,t)$ and $0 < r < r_0$, where r , z , and t are the radial, axial and time variables, respectively. Here k and α are the thermal conductivity and thermal diffusivity of the substrate, respectively, and g is the volumetric heat source which is given by

$$g = -\frac{\partial I_{ip}}{\partial z} + \frac{\partial I_{rp}}{\partial z}. \quad (7)$$

The boundary conditions are

$$T = T_v \quad \text{at } z = s(r,t), \quad (8a)$$

$$-k \frac{\partial T}{\partial z} + I_a = \frac{T - T_0}{R_{\text{th}}} \quad \text{at } z = d - s(r,t), \quad (8b)$$

$$\frac{\partial T}{\partial r} = 0 \quad \text{at } r = 0, \quad (8c)$$

$$-k \frac{\partial T}{\partial r} = \frac{k}{\delta_{\text{poly}}} (T - T_0) \quad \text{at } r = r_0, \quad (8d)$$

where T_v is the vaporization point. T_0 is the ambient temperature. I_a is the laser irradiance absorbed by the copper surface, $I_a = (1 - R_{\text{Cu}})I_i \exp\{-\mu[d - s(r,t)]\}$. R_{th} is the thermal resistance of the copper layer and the polymer layer beneath the copper layer.

$$R_{\text{th}} = \frac{\delta_{\text{Cu}}}{k_{\text{Cu}}} + \frac{\delta_{\text{poly}}}{k}, \quad (9)$$

where δ_{Cu} and k_{Cu} are the thickness and thermal conductivity of the copper layer, respectively. δ_{poly} is the thickness of the thermal diffusion depth in the underlying polymer layer.

The liquid temperature may exceed the boiling point of the polymer to form a liquid-vapor interface. This may lead to the formation of a Knudsen layer causing discontinuities in the temperature, density, and vapor velocity.¹⁷ The Knudsen layers are formed under extremely high vaporization conditions. During the microvia drilling in polymers, the extremely high vaporization conditions need to be avoided in order to prevent any thermal damage to the substrate due to excessive heating. The Knudsen layer would not exist under such conditions. The liquid layer, however, is considered to vaporize almost instantaneously since the layer is extremely thin. This solid-to-vapor phase transformation is considered in the model through the latent heat of sublimation in the Stefan condition. The Stefan condition at the solid-vapor interface is²⁸

$$k \frac{\partial T}{\partial z} \left\{ 1 + \left[\frac{\partial s(r,t)}{\partial r} \right]^2 \right\} = \rho L_v \frac{\partial s(r,t)}{\partial t} \quad \text{at } z = s(r,t), \quad (10)$$

where L_v , ρ , and C_p are the heat latent of vaporization, density, and specific heat of the polymer, respectively.

Since a large amount of thermal energy is removed from the drilling zone by the vapor, a quasisteady state exists for this drilling process. There is a time lag to establish the quasisteady process as the surface temperature approaches the vaporization point. However, since the Stefan number St is very small, i.e., $St = C_p(T_v - T_0)/L_v \rightarrow 0$, this time lag is very short and can be neglected. Therefore the quasisteady state approximation can be applied as soon as the laser irradiation begins.²⁸

Since the laser beam is incident on the substrate vertically in the z direction, much of the laser energy will be transferred to the substrate in the z direction. So the heat conduction will be dominant in the z direction compared to the r direction. Thus Eq. (6) can be simplified to the following form under the quasisteady state approximation:

$$\frac{\partial^2 T}{\partial z^2} + \frac{g}{k} = - \frac{1}{\alpha} \frac{\partial T}{\partial z} \frac{\partial s(r,t)}{\partial t}. \quad (11)$$

This equation is solved subject to the boundary and Stefan conditions given by Eqs. (8) and (10) to obtain the temperature distribution and the drilling front profile.

III. METHOD OF SOLUTION

The general problem of the motion of any phase boundary with heat conduction is known as the Stefan problem. Different analytical methods are used to solve the Stefan problem under a variety of phase change conditions.²⁹⁻³² In this study, Eq. (11) can be integrated with respect to z directly to obtain the following expression for the temperature distribution in the substrate:

$$T(r,z,t) = \frac{C_1}{\rho C_p} \frac{1}{\partial s(r,t)/\partial t} + C_2 \exp\{-[\partial s(r,t)/\partial t]z/\alpha\} + \frac{1}{\rho C_p} \frac{I_{ip}}{[\partial s(r,t)/\partial t] - \alpha\mu} - \frac{1}{\rho C_p} \frac{I_{rp}}{[\partial s(r,t)/\partial t] + \alpha\mu}, \quad (12)$$

where C_1 and C_2 are integral constants and are functions of r and t . By substituting Eq. (12) into boundary conditions (8a) and (8b), C_1 and C_2 can be expressed as

$$C_2 = \frac{T_v - T_0 - I_a R_{th} - I_i \frac{\alpha}{\frac{\partial s(r,t)}{\partial t} - \alpha\mu} \left(\frac{1}{k} + \left(R_{th}\mu - \frac{1}{k} \right) \exp\{-\mu[d - s(r,t)]\} \right) + I_r \frac{\alpha}{\frac{\partial s(r,t)}{\partial t} + \alpha\mu} \left(\frac{1}{k} \exp\{-\mu[d - s(r,t)]\} - \left(R_{th}\mu + \frac{1}{k} \right) \right)}{1 - \exp\left[- \frac{\partial s(r,t)}{\partial t} \frac{d - s(r,t)}{\alpha} \right] \left[1 - \rho C_p R_{th} \frac{\partial s(r,t)}{\partial t} \right]},$$

and

$$C_1 = \rho C_p \frac{\partial s(r,t)}{\partial t} \left(T_v - \frac{1}{\rho C_p} \frac{I_i}{\frac{\partial s(r,t)}{\partial t} - \alpha\mu} + \frac{1}{\rho C_p} \frac{I_r \exp\{-\mu[d - s(r,t)]\}}{\frac{\partial s(r,t)}{\partial t} + \alpha\mu} - C_2 \right).$$

Now substituting Eq. (12) into the Stefan condition (10), a partial differential equation for $s(r,t)$ is obtained as follows:

$$\frac{\partial s(r,t)}{\partial t} = A_1 I_i + A_2 I_i s(r,t) + \left[A_3 \frac{\partial s(r,t)}{\partial t} + A_1 I_i + A_2 I_i s(r,t) \right] \left[\frac{\partial s(r,t)}{\partial r} \right]^2, \quad (13)$$

which can be rewritten as

$$\frac{\partial s(r,t)}{\partial r} = f[r,t,s(r,t)], \quad (14)$$

where

$$A_1 = \frac{k R_{th} \mu [2 \exp(-\mu d) - 1 - \exp(-2\mu d)] + 1 - \exp(-2\mu d)}{\rho [C_p(T_v - T_0) + L_v]},$$

$$A_2 = - \frac{A_1}{d},$$

$$A_3 = - \frac{\rho C_p (T_v - T_0)}{\rho [C_p(T_v - T_0) + L_v]},$$

and

$$f[r, t, s(r, t)] = \left\{ \frac{[\partial s(r, t)/\partial t] - A_1 I_i - A_2 I_i s(r, t)}{A_3 [\partial s(r, t)/\partial t] + A_1 I_i + A_2 I_i s(r, t)} \right\}^{1/2}.$$

The drilling front is considered to be symmetric at $r=0$, so $\partial s(r, t)/\partial r=0$ and then Eq. (13) can be written as

$$\frac{\partial s_0(r, t)}{\partial t} = A_1 I_i + A_2 I_i s_0(r, t) \quad \text{at } r=0. \quad (15)$$

By using the integrating factor $\exp(\int_0^t -A_2 I_i dt)$, Eq. (15) can be solved to obtain

$$s_0(r, t) = \frac{\int_0^t A_1 I_i \exp\left(\int_0^t -A_2 I_i dt\right) dt}{\exp\left(\int_0^t -A_2 I_i dt\right)}. \quad (16)$$

Since a solution of $s(r, t)$ is known at $r=0$, Eq. (14) can now be solved by the method of successive approximation,³³

$$s_1(r, t) = s_0(r, t) + \int_0^r f[r', t, s_0(r', t)] dr',$$

$$s_2(r, t) = s_0(r, t) + \int_0^r f[r', t, s_1(r', t)] dr',$$

⋮

$$s_n(r, t) = s_0(r, t) + \int_0^r f[r', t, s_{n-1}(r', t)] dr'.$$

As n increases indefinitely, the sequence of function $s_n(r, t)$ tends to the exact solution of Eq. (14).

The results show that the iteration converges rapidly. From the calculated result, it is found that the difference between $s_1(r, t)$ and $s_0(r, t)$ is very small. So $s_1(r, t)$ is taken as the approximate solution to Eq. (14),

$$s(r, t) = s_0(r, t) + \int_0^r f[r', t, s_0(r', t)] dr'. \quad (17)$$

After calculating the drilling front profile $s(r, t)$, the temperature distribution can be obtained by substituting Eq. (17) into Eq. (12).

IV. RESULTS AND DISCUSSION

The results are obtained for a particular type of polymeric substrate whose properties are listed in Table I. The absorption coefficient of this substrate is listed for a CO₂ laser of wavelength 9.3 μm, as opposed to the conventional 10.6 μm, because of higher absorptivity of the polymer of interest at this slightly lower wavelength. The thicknesses of the polymer layer and the copper layer are 30 and 15 μm, respectively. The radius of the incident laser beam is taken as 20 μm, which is expected to produce microvias with a radius of 20 μm. The repetition rate of laser pulses is 20 KHz, which corresponds to a period of 50 μs. The laser powers and pulse-on times are varied to examine their effects on the volumetric heating.

TABLE I. The material properties of the polymer.

Thermal conductivity	0.3 W/m K
Specific heat	1.0×10^3 J/kg K
Density	1.2×10^3 kg/m ³
Glass transition temperature	363 K
Thermal decomposition point	583 K
Latent heat of vaporization	1.72 MJ/kg
Reflectance	0.3
Absorption coefficient at wavelength 9.3 μm	1.03×10^5 m ⁻¹
Thermal expansion coefficient	11.2×10^{-5} K ⁻¹
Elastic modulus	0.62 GPa
Poisson ratio	0.35

A. Overheating and thermal stresses

The temperature distributions along the z direction at $r=0$ are presented in Fig. 3 for different laser powers which correspond to different irradiances. Because of the Gaussian beam profile, the maximum laser irradiance (I_0) occurs at the center of the beam ($r=0$) and this produces maximum temperature at $r=0$ on a given plane of fixed depth. For low laser irradiances the maximum temperature occurs at the drilling front. There is a definite temperature gradient in the z direction within the polymer layer. The temperature gradient, however, is very small in the copper layer because of its high thermal conductivity (~ 390 W/m K), which is about 1000 times higher than that of the polymer substrate. The volumetric heating becomes important at high laser irradiances. For $I_0 \leq 1$ kW/cm² the overheating inside the polymer can be neglected. For $I_0 = 1.2$ MW/cm² the maximum temperature inside the polymer is 2630 K which is much higher than the vaporization point 583 K.

As the drilling process progresses, the drilling front moves downward in the z direction and thus the calculation region decreases as time increases. The temperature distribution at $r=0$ is presented in Fig. 4 for four different times after the beginning of laser irradiation. The average power of the Gaussian laser beam = 3 W, pulse-on time = 20 μs, and

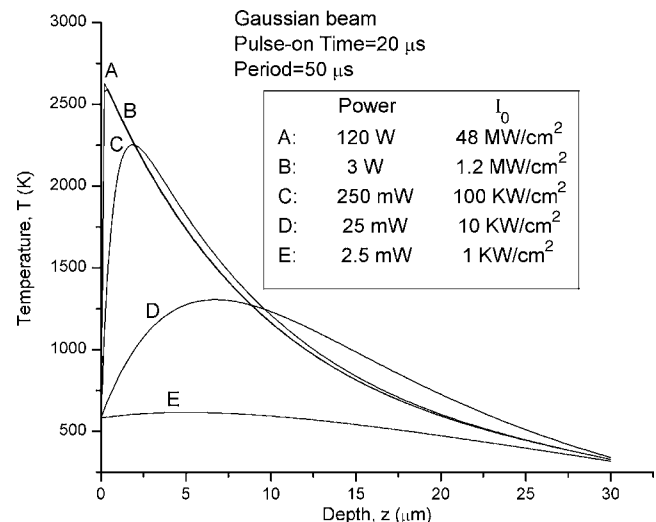


FIG. 3. Temperature distribution at different maximum laser irradiances of Gaussian beams for pulse-on time = 20 μs, period = 50 μs, and time $t = 0$ μs.

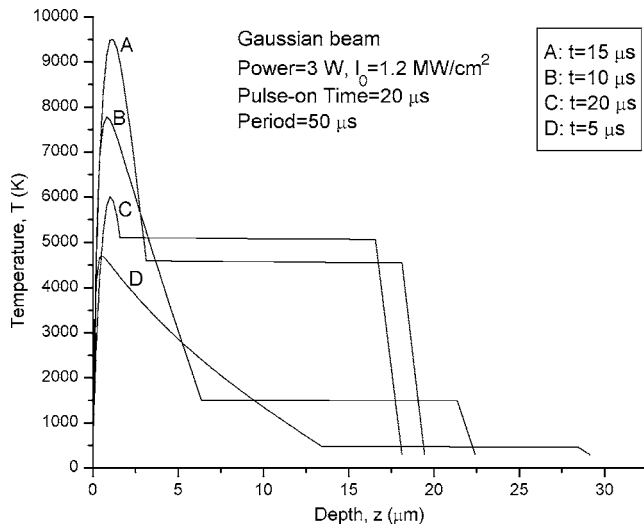


FIG. 4. Temperature distribution at different times after laser irradiation begins for a Gaussian beam of $P=3$ W, pulse-on time= $20 \mu\text{s}$, and period= $50 \mu\text{s}$.

period= $50 \mu\text{s}$. As the irradiation time increases, the maximum temperature inside the polymer increases at first because of heat accumulation. As the drilling process progresses, however, the thickness of the polymer to absorb the laser energy reduces and the laser energy reflected by the copper layer increases with time. When the heat loss is larger than the heat accumulation, the temperature of the polymer drops and that is why the temperature of the polymer is found to be less at $t=20 \mu\text{s}$ than at $t=15 \mu\text{s}$. The maximum temperature exceeds the vaporization point by 8914 K for irradiation time $t=15 \mu\text{s}$, which is very high for any polymer to maintain its thermochemical and thermomechanical integrities. There will be explosive removal of materials. In this study, the development of overheating and the onset of polymer rupture due to thermal stresses are studied.

Since the temperature difference in the z direction is much larger than the other directions, only the thermal stress in the z direction is considered. The axial stress around the heated polymer is given by³⁴

$$\sigma_{zz} = \frac{\beta E(T - T_0)}{1 - \nu}, \quad (18)$$

where β is the thermal expansion coefficient, E is the elastic modulus, and ν is the Poisson ratio. The thermal stress along the z direction within one pulse-on time is shown in Fig. 5 for a Gaussian laser with an average power of 3 W, pulse-on time of $20 \mu\text{s}$, and period of $50 \mu\text{s}$. The thermal stress is proportional to the temperature as evident in Eq. (18). The yield stress of the polymer is 0.5 GPa, which is shown as a horizontal dash line in Fig. 5. The region where the value of thermal stress exceeds the yield stress will rupture or explode.

Figure 6 shows the location, i.e., the depth from the drilling front at $r=0$, where the maximum temperature occurs. As the laser irradiation time increases, the depth of the point of maximum temperature (D_m) first increases and then decreases. This is due to two effects: (a) the drilling speed and consequently the material removal rate and (b) the reflection

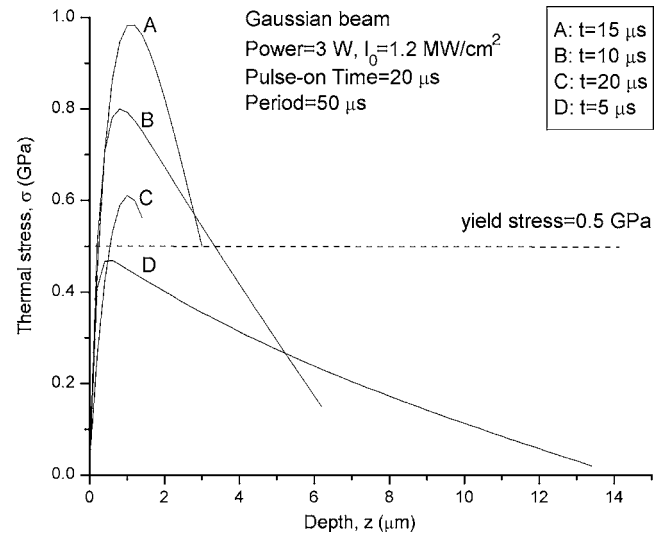


FIG. 5. Thermal stress distribution along the z direction at different times after laser irradiation begins for a Gaussian beam of $P=3$ W, pulse-on time= $20 \mu\text{s}$, and period= $50 \mu\text{s}$.

of laser power by the copper layer. As the energy absorbed inside the polymer increases, D_m increases at first, and then as the drilling proceeds, the thickness of the polymer to absorb the laser energy reduces and consequently the value of D_m decreases. On the other hand, D_m decreases as the pulse-on time decreases because decreasing the pulse-on time increases the laser irradiance for a given laser average power which increases the drilling speed. Therefore the thickness of the polymer decreases leading to reduced values of D_m . The reflective effect of the copper layer is discussed in the following section.

B. Drilling depth profile

1. Effect of embedded copper layer

The drilling speed is greatly reduced due to the buried copper layer. It can be seen in Fig. 7 that after $20 \mu\text{s}$ of irradiation with a Gaussian beam of $P=3$ W, pulse-on time

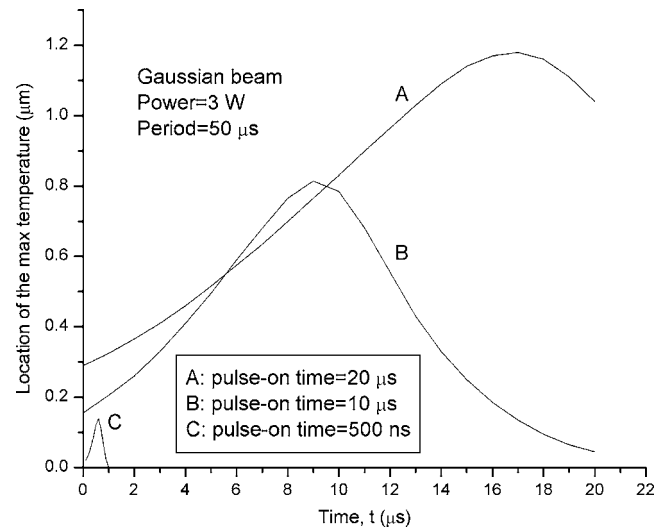


FIG. 6. The location of the maximum temperature from the drilling front surface at $r=0$ for $P=3$ W, and period= $50 \mu\text{s}$.

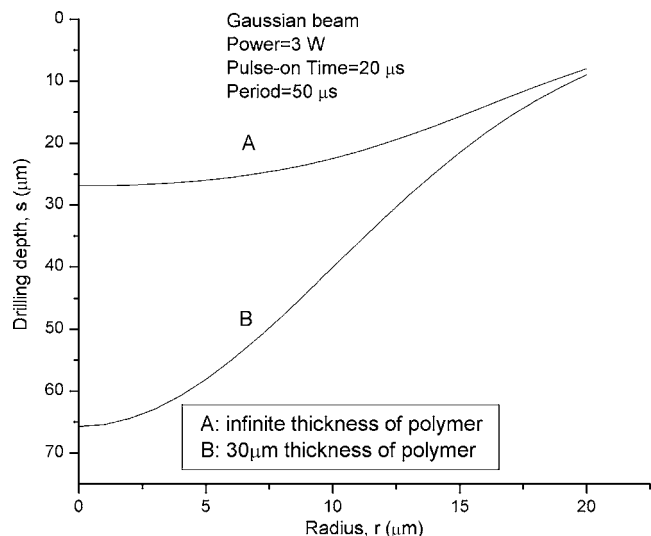


FIG. 7. The difference of drilling depth profile between infinite thick polymer and 30 μm thick polymer for the same Gaussian beam of $P=3$ W, pulse-on time=20 μs, period=50 μs, and time $t=20$ μs.

=20 μs, and period=50 μs, the drilling depth is much larger for an infinitely thick polymer substrate than for a 30 μm thick polymer layer containing a buried copper layer. This is due to the energy loss through heat conduction and reflection of the laser beam by the copper layer.

The drilling time, which is defined as the time required for the drilling front to reach the copper layer, is a sum of the times necessary to complete three events: (a) time required to heat up the substrate surface temperature to the vaporization point, (b) vaporization time during pulse-on time, and (c) vaporization time during pulse-off time due to overheating inside the polymer. The heating time due to effect (a) was obtained from a two-dimensional heat conduction model.²⁶ The maximum depth drilled during the pulse-off time can be estimated by the following expression:

$$\Delta s = \frac{1}{L_v} \int_0^{dp-s} C_p(T - T_v) dz. \tag{19}$$

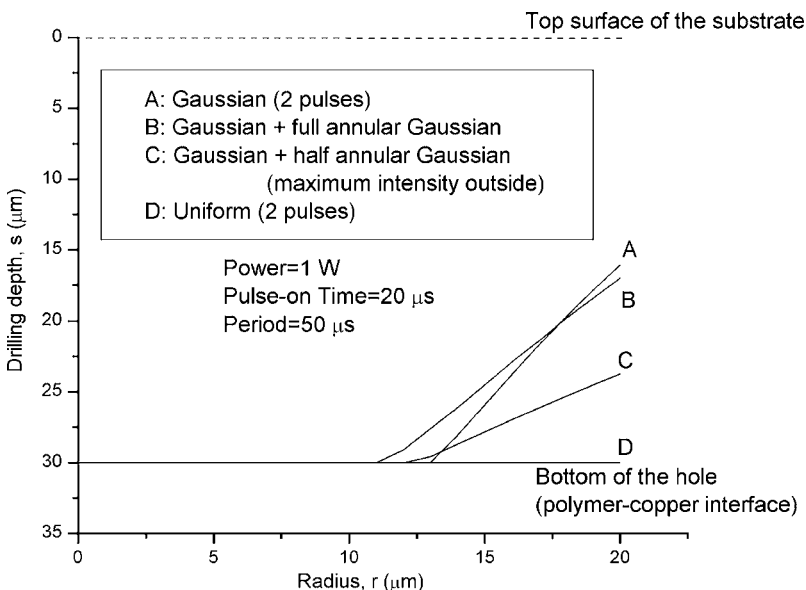


FIG. 9. The drilling depth after two pulses of laser irradiation for different beam profiles of $P=1$ W, pulse-on time=20 μs, and period=50 μs.

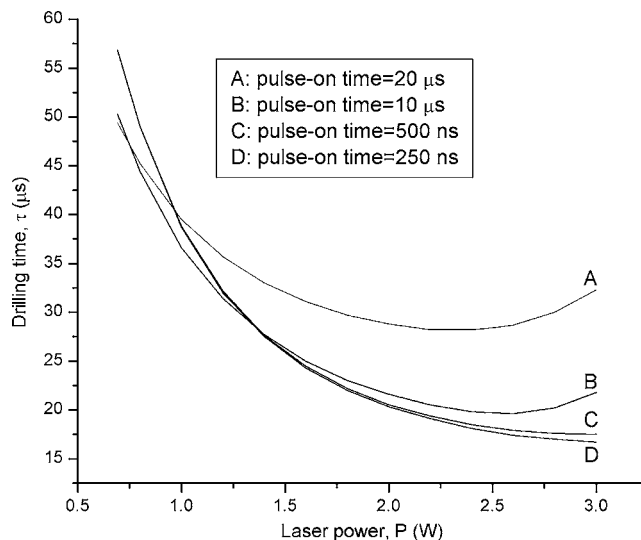


FIG. 8. The drilling time as a function of laser power for different pulse-on time Gaussian beams of period=50 μs.

It should be noted that the drilled depth obtained from Eq. (19) would be less than the actual depth due to the conduction heat loss in the polymer layer although the thermal conductivity of the polymer is small.

The drilling times are presented in Fig. 8 as a function of laser power for different pulse-on times. The laser irradiance increases with increasing laser power and this increases the drilling speed causing a reduction in the drilling time. However, the drilling time increases after a critical laser power is reached because the thickness of the polymer decreases below its absorption length (l_v) in a single pulse of high irradiance laser beams. This allows the laser beam to pass through the polymer layer to reach the copper surface where it is reflected back to the ambient. Thus much of the laser energy is lost instead of being used for drilling the polymer and consequently the drilling time increases. This energy loss also diminishes the magnitude of the maximum temperature due to overheating inside the polymer, resulting in reduced

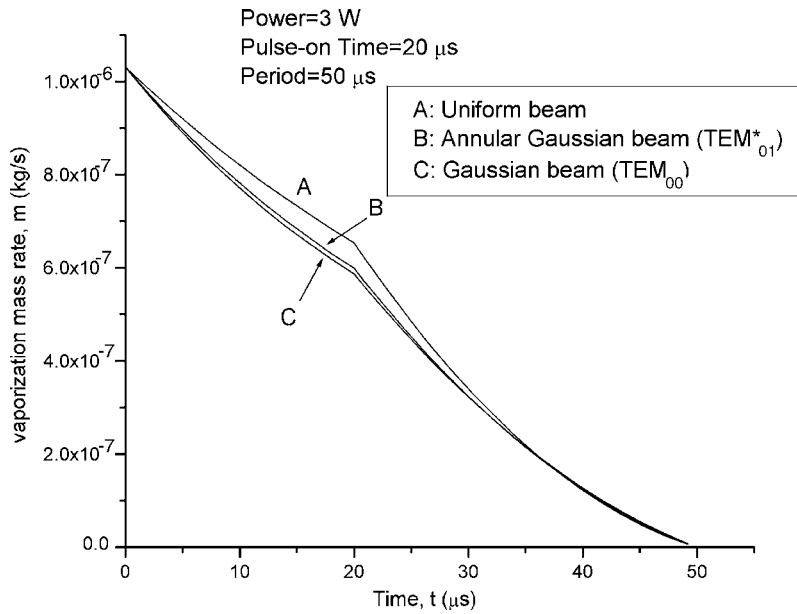


FIG. 10. The mass removing rate variation with times after laser irradiation begins for different laser beam profiles of $P=3$ W, pulse-on time= $20 \mu\text{s}$, and period= $50 \mu\text{s}$.

drilling speed during the pulse-off time. So the total drilling time will increase due to the energy loss by reflection and the reduction in overheating.

2. Drilling front profile for different laser beam profiles

For low laser power, the residue exists even after two pulses of laser irradiation. The amount of residue is, however, different for different combinations of the laser beam shape. The drilling depth after two pulses of laser irradiation is presented in Fig. 9 for different beam shapes with the same laser power of 1 W and the same period of $50 \mu\text{s}$. For curves A–C, the first irradiation is with a Gaussian beam and then the second irradiation is applied with a Gaussian beam, a full Gaussian annular beam (with the maximum irradiance being at the central circle of the annulus), and a half Gaussian annular beam (with the maximum irradiance being at the outer radius of the annulus), respectively. When both irradiations are due to a laser beam of uniform irradiance profile, the thickness of the residue is approximately to zero at the bottom of the hole (curve D in Fig. 9). When the first irradiation is with a Gaussian beam, the second irradiation should be with a half Gaussian annular beam to achieve the minimum amount of residue at the bottom of the hole (curve C in Fig. 9).

To compare the drilling efficiency of these three beam profiles, the mass removal rate through vaporization is calculated as follows:

$$\dot{m} = \int_0^{r_0} \rho \frac{\partial s(r,t)}{\partial t} 2\pi r dr, \quad (20)$$

and the results are presented in Fig. 10. For each beam profile, the mass removal rate is large at the beginning of the drilling process and then the rate reduces with time as the drilling front approaches towards the copper layer. This is because the thickness of the polymer absorbing the laser energy is reduced and the laser energy reflected by the copper layer is increased. During the pulse-off time, the mass re-

moval rate drops sharply to zero. The mass removal rate for a uniform beam profile is almost always higher than that for the Gaussian or the annular Gaussian beam profiles. It should be noted that the area below each curve in Fig. 10 is the total mass removed during the drilling process. The total mass removed by the uniform laser beam profile is the largest.

V. CONCLUSION

A thermal model with volumetric heating source is presented to analyze the microvia drilling process in polymeric substrates.

- (1) Because of volumetric heating, an overheated region is formed inside the polymer for laser irradiances larger than 1 kW/cm^2 . The maximum internal temperature of polymer increases as the laser irradiance increases.
- (2) The depth of the point of maximum temperature from the drilling front first increases and then decreases as the drilling process progresses. This depth also decreases as the laser pulse-on time decreases.
- (3) As the drilling front approaches the bottom of the hole the volume of the polymer that absorbs the laser energy decreases and the laser energy reflected by the copper layer increases. Consequently, the drilling speed decreases. Residues are formed at the bottom of the hole. These residues may be removed using lasers of different beam profiles.

ACKNOWLEDGMENTS

This work was supported by AppliCote Associates, LLC and Intel Corporation—Assembly and Technology Development.

¹L. Migliore, *Laser Materials Processing* (Marcel Dekker, New York, 1996), p. 67.

²Y. K. Godovsky, *Thermophysical Properties of Polymers* (Spring-Verlag, New York, 1992), pp. 28–40.

³N. Arnold, N. Bityurin, and D. Bauerle, *Appl. Surf. Sci.* **138**, 212 (1999).

- ⁴L. G. Hector and R. B. Hetnarski, *Thermal Stresses IV* (Elsevier, New York, 1996), pp. 453–531.
- ⁵S. Noguchi, E. Ohmura, and I. Miyamoto, Proc. SPIE **4830**, 46 (2003).
- ⁶V. I. Mazhukin, I. Smurov, and G. Flamant, J. Appl. Phys. **78**, 1259 (1995).
- ⁷J. F. Li, L. Li, and F. H. Stott, Int. J. Heat Mass Transfer **47**, 1159 (2004).
- ⁸V. I. Mazhukin, I. Smurov, C. Surry, and G. Flamant, Appl. Surf. Sci. **86**, 7 (1995).
- ⁹D. Von Der Linde, N. Fabricius, B. Danielzik, and T. Bonkhofer, Mater. Res. Soc. Symp. Proc. **74**, 103 (1987).
- ¹⁰T. Hirogaki, E. Aoyama, H. Inoue, K. Ogawa, S. Maeda, and T. Katayama, Composites, Part A **32**, 963 (2001).
- ¹¹T. Kawamura, H. Akahoshi, and K. Arai, IEEE Trans. Electron. Packag. Manuf. **24**, 39 (2001).
- ¹²S. Sankaranarayanan and A. Kar, J. Phys. D **32**, 777 (1999).
- ¹³V. I. Mazhukin, V. V. Nossov, and I. Smurov, Thin Solid Films **453**, 353 (2004).
- ¹⁴C. H. Fan, J. Sun, and J. P. Longtin, Int. J. Heat Mass Transfer **124**, 275 (2002).
- ¹⁵C. Zhang, S. Bet, I. A. Salama, N. R. Quick, and A. Kar, Symposium Packaging of Electronic and Photonic Systems, InterPack, 2005 (American Society of Mechanical Engineers, New York, 2005).
- ¹⁶A. Kar, T. Rockstroh, and J. Mazumder, J. Appl. Phys. **71**, 2560 (1992).
- ¹⁷A. Kar and J. Mazumder, Phys. Rev. E **49**, 410 (1994).
- ¹⁸A. Kar, J. E. Scott, and W. P. Latham, J. Appl. Phys. **80**, 667 (1996).
- ¹⁹J. Xie and A. Kar, J. Appl. Phys. **81**, 3015 (1997).
- ²⁰W. Pecharapa and A. Kar, J. Phys. D **30**, 3322 (1997).
- ²¹F. W. Dabby and U. C. Paek, IEEE J. Quantum Electron. **QE-8**, 106 (1972).
- ²²E. N. Sobol and N. G. Petrovskaya, Supercond. Sci. Technol. **6**, 67 (1993).
- ²³C. L. Chan and J. Mazumder, J. Appl. Phys. **62**, 4579 (1987).
- ²⁴B. Wunderlich, *Thermal Analysis of Polymeric Materials* (Springer, New York, 2005), p. 576.
- ²⁵D. R. Poirier and G. H. Geiger, *Transport Phenomena in materials Processing* (TMS, Warrendale, Pennsylvania, 1994), pp. 29–34.
- ²⁶Y. R. Luo, *Handbook of Bond Dissociation Energies in Organic Compounds* (CRC, New York, 2003), pp. 61 and 130.
- ²⁷C. Zhang, I. A. Salama, N. R. Quick, and A. Kar, Symposium of ICALEO 2005 (Laser Institute of America, Orlando, FL, 2005), pp. 404–411.
- ²⁸V. Alexiades and A. D. Solomon, *Mathematical Modeling of Melting and Freezing Processes* (Hemisphere, Washington DC, 1993), p. 106.
- ²⁹T. R. Goodman and J. J. Shea, ASME J. Appl. Mech. **27**, 16 (1960).
- ³⁰D. W. Jordan, Br. J. Appl. Phys. **12**, 14 (1961).
- ³¹V. N. Volkov and V. K. Li-Orlov, Heat Transfer-Sov. Res. **2**, 41 (1970).
- ³²J. G. Andrews and D. R. Atthey, J. Inst. Math. Appl. **15**, 59 (1975).
- ³³E. L. Ince, *Ordinary Differential Equations* (Dover, New York, 1956), p. 63.
- ³⁴A. Kar and M. D. Langlais, Opt. Quantum Electron. **27**, 1165 (1995).